Modeling the influence of fiber undulation in a filament-wound composite tube under radial crushing load

Komala, Ivan; van Campen, Julien; Peeters, Daniël; Heimbs, Sebastian

DOI
10.1016/j.mfglet.2024.12.003

Publication date
2025

Document Version
Final published version

Published in
Manufacturing Letters

Manufacturing Letters 43 (2025) 51–54

Contents lists available at ScienceDirect

Manufacturing Letters

journal homepage: www.elsevier.com/locate/mfglet

Letters

Modeling the influence of fiber undulation in a filament-wound composite tube under radial crushing load

Ivan Komala [a,b,c,*], Julien van Campen [a,b], Daniël Peeters [a,b], Sebastian Heimbs [a,c]

[a] Cluster of Excellence SE²A – Sustainable and Energy-Efficient Aviation, Technische Universität Braunschweig, Braunschweig 38108, Germany
[b] Department of Aerospace Structures & Materials, Faculty of Aerospace Engineering, Delft University of Technology, Kluyverweg 1, Delft 2629 HS, The Netherlands
[c] Institute of Aircraft Design and Lightweight Structures (IFL), Technische Universität Braunschweig, Hermann-Blenk-Straße 35, Braunschweig 38108, Germany

ARTICLE INFO

Article history:
Received 2 September 2024
Received in revised form 3 December 2024
Accepted 6 December 2024
Available online 9 January 2025

Keywords:
Filament winding
Fiber undulation
Radial stiffness
Radial crushing

ABSTRACT

This study investigates a filament-wound tube model incorporating fiber undulation from the filament winding process. The model was analyzed using the finite element method in the linear regime, then compared with the shell model and radial crushing experiment. Results showed that the solid model predicts the radial compression stiffness with a higher level of accuracy than the shell model due to the inclusion of the fiber undulation feature. This model is a first step towards the development of a composite pressure vessel model where fiber undulation is more frequent, and also for predicting failure initiation and damage propagation.

1. Introduction

The widespread use of composite structures necessitates understanding how manufacturing processes affect their performance. Filament winding is the preferred method for producing axisymmetric composite geometries such as pressure vessels or tubes due to its high fiber content, minimum void introduction, high accuracy, and automation potential. Even though the performance of the composite parts is primarily based on the material properties, other factors such as fiber angles [1], stacking sequence [2,3] and the impact of the filament winding process such as gaps due to fiber overlap [4] and thickness variation [5] can also influence its performance.

The objective of this study is to gain a deeper understanding of the effect of the actual fiber path and undulation on the mechanical performance of a filament-wound structure. Radial compressive loads are commonly introduced in underground pipes [6], underwater pipes, and also used for the oil offloading hoses [7]. Under this load, previous studies showed that the winding pattern affects tube stiffness [8,9], and failure prediction was studied [10]. However, previous studies did not account for fiber undulation.

In this research the finite element (FE) method was used to model a filament-wound composite tube with undulations. This paper starts with modeling (Section 2), followed by the experimental method (Section 3), and the models are compared to experiments (Section 4). The effect of fiber undulation on the compressive stiffness under radial crushing load was observed.

2. Filament-wound composite tube modeling

The samples were manufactured using a filament winder from McClean Anderson, on a 106 mm diameter aluminum mandrel. CADWIND software generated the path with a 1/1 winding pattern selected for all the samples due to its optimum fiber coverage with the chosen winding parameters. In filament winding, the winding pattern is directly connected to the locations of fiber placement and fiber overlap. The first number in the winding pattern represents the number of wraps around the mandrel before the turnaround, visually shown by the number of diamonds around the tube circumference (see Fig. 1), and the second number indicates the number of fiber widths skipped for each path [11].

T700 Carbon fiber from Toray Composite Materials Inc. and epoxy resin by Advanced Material Systems (AMS) were used and cured according to the manufacturer's specifications. Both ends of the samples were cut into the required length where one diamond shape was found, and polished at both ends to remove burrs. This ensured an identical structure to the numerical model and eliminated the effect of fiber slippage at the turnaround point.

* Corresponding author at: Department of Aerospace Structures & Materials, Faculty of Aerospace Engineering, Delft University of Technology, Kluyverweg 1, Delft 2629 HS, The Netherlands
E-mail address: i.komala@tudelft.nl (I. Komala).

https://doi.org/10.1016/j.mfglet.2024.12.003

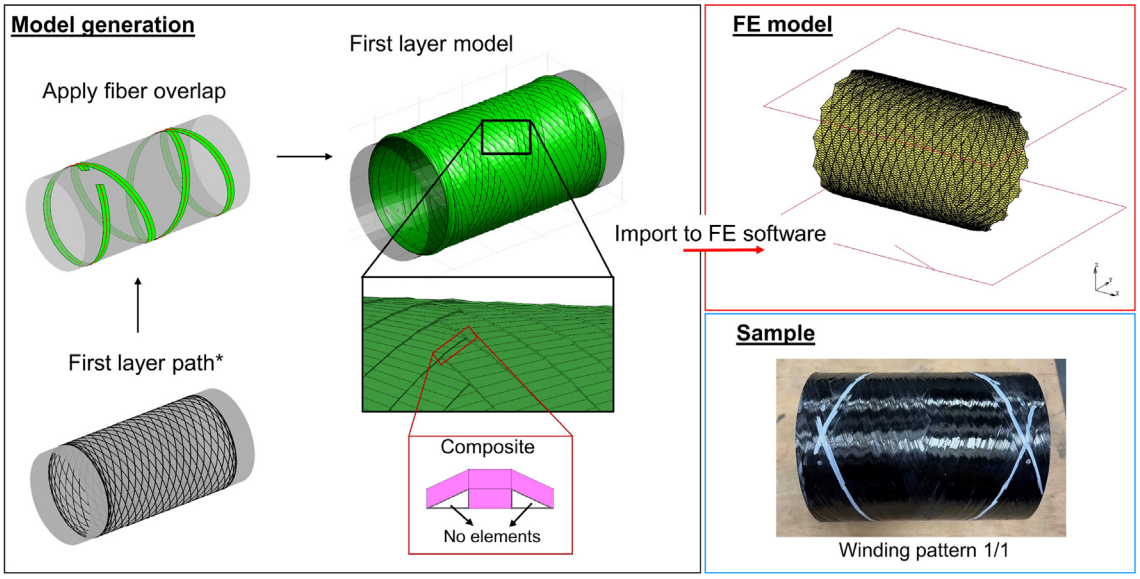

Fig. 1. Schematic representation of modeling procedure for filament-wound composite tube and a manufactured sample.

With a controlled winding speed, mandrel rotation speed and fiber tension, the fiber angle at the cylindrical part can be assumed to be constant. Material properties were taken from AMS's tensile test experiment shown in Table 1.

A solid-element FE model based on the ideal winding path of resin-impregnated fibers and their directional properties was developed in this study. The fiber path calculation was based on a previous study about non-geodesic filament winding path [12] with a friction coefficient of 0.2 for wet winding [13]. The trajectories used in this article were based on polar coordinates, and the shell of revolution can be expressed by

$$S(\phi,\rho) = \{\rho cos\phi, \rho sin\phi, z(\phi)\}$$

where ϕ is the angular coordinate and ρ represents the radial distance. The filament winding parameters were based on manufacturing default using 8.8 mm bandwidth and 64% fiber volume fraction, creating 0.234 mm ply thickness for every layer. Applying these inputs to the formulation, the path for a layer can be calculated depending on the bandwidth, winding pattern, and fiber coverage.

The main difference between composite modeling using shell elements and this method is that the shell model does not include the effect of fiber undulation from the filament winding process. While some argue that gaps can be eliminated by ensuring full fiber coverage [14], or by resin transverse flow during the consolidation step [15], the overlaps between fibers remain. This potentially causes non-uniform thickness and fiber waviness in the subsequent layers that affect the structure's stiffness. In this research, the fiber overlap algorithm was applied based on the node-to-node comparison, overlap exists when the fiber in the current winding path:

- self-intersects, between the first half and second half
- intersects with the previous paths

For every satisfied condition, the node's location at ρ-axis was increased by one ply thickness. An input file for further processing in the FE software was generated by combining the updated nodes to become 3D solid elements. MSC Marc software was used for the finite element analysis (FEA). The resolution of the nodes was increased to avoid element penetration due to coarse elements and to enhance the accuracy of the results. The solid model (8-node solid element CHEXA, 2x9 mm) thickness was based on the overlap algorithm, while the shell model (4-node shell element CQUAD4, 2x9 mm) had uniform thickness taken from the average thickness of manufactured samples.

The stacking sequence of $[\pm 70_3]$ was selected based on the manufactured samples. The node locations for the following layers were based on the previous layer. All layers with the same angle had the same fiber path to simplify the model. The layer-to-layer contact was assumed to be in perfect bonding. This approach was used to avoid errors during the analysis due to element distortion and edge effects. Some assumptions were made for the fiber location formulation of this model:

- no fiber slip during the winding
- filament winding parameters were in ideal condition, thus exact angle throughout the path
- gaps exist as empty spaces and are not filled with matrix

The generated model was imported to the FE software and applied with a local coordinate system for each element that followed the fiber path direction. The failure criterion and damage propagation were not included in this model due to the limitation of available material data. Current model boundary conditions were based on the experiment shown in Fig. 2. This experiment represents a study case of an underground pipe where the soil provides lateral support but allows axial movement, thus it can freely deform, and the radial crushing loads are from the ground surface. The composite tube was placed in the middle of two rigid surfaces, where the bottom surface was fixed and the top surface descended. The contact between the tube and both rigid surfaces is a touching contact with a friction coefficient of 0.1 to constrain the tube movement.

Table 1
Material properties of T700/Epoxy.

E_1 (MPa)	E_2 (MPa)	v_{12}	G_{12} (MPa)	G_{13} (MPa)	G_{23} (MPa)
149,000	4,790	0.324	2,360	2,360	1,780

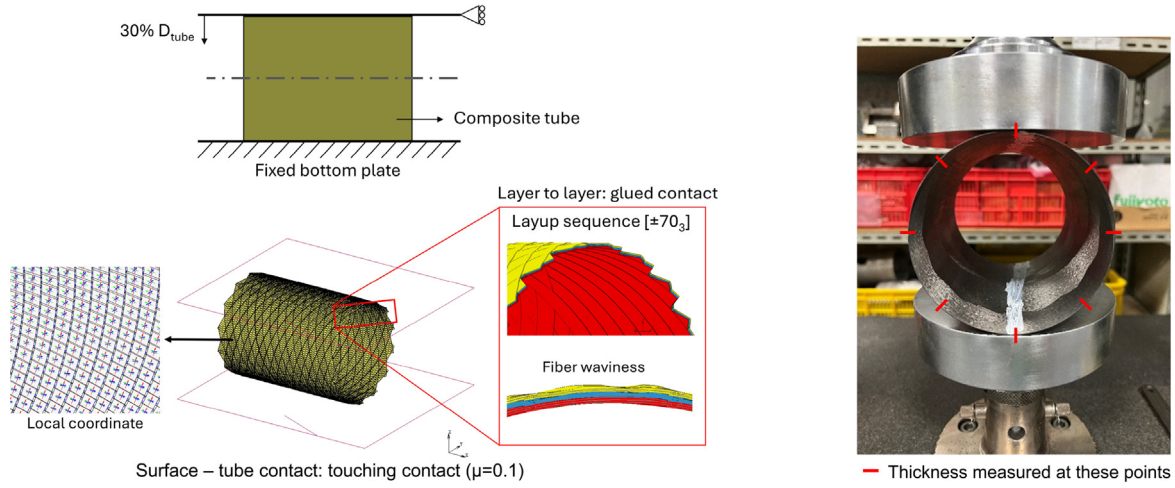

Fig. 2. Left: Finite element model and boundary conditions. Right: experimental setup.

3. Experimental method

This experiment followed ASTMD2412 [16]. Five composite tubes were manufactured under identical parameters and conditions. The wall thickness of each tube was measured at eight points at each tube end according to ASTMD2122 [17], with the average wall thickness of 1.52±0.12 mm. The experimental setup is shown in Fig. 2.

An Instron 3412 universal testing machine was used to conduct the radial crushing test. The upper plate movement has a constant rate of 12.5 mm/min and the loading plate diameter used was 150 mm. The ambient temperature was kept constant at 25°C to avoid thermal effects. The thinnest wall was positioned at the top and the moving plate had to be in contact with the sample with no more than the load necessary to hold it in place. The plate stopped moving after 35 mm. The force and displacement of the plate were measured and the failure was observed but not investigated further.

4. Results & discussion

The main observation in Fig. 3 was the composite tube stiffness in the elastic region at 15 mm deflection. The experiments showed an average stiffness of 116.57±9.1 N/mm while the model including fiber undulation predicted 113.62 N/mm (2.53% error) and the shell model, without fiber undulation, predicted 123.56 N/mm (6% error). The FEA of the solid model was stopped at 19.6 mm deflection when the tube's compressive stress had reached 1450 MPa which was assumed the maximum [18].

All results aligned closely for the first 5 mm of deflection, but deviations appeared afterward due to imperfections in the manufacturing process, especially undulations that caused waviness and non-uniform thickness. These factors were absent in the shell model, which assumed a uniform thickness resulting in slightly over-predicting the stiffness. In contrast, the solid model accounts for fiber undulation, which led to gaps and thickness variation which reduced the stiffness, as observed during the experiments.

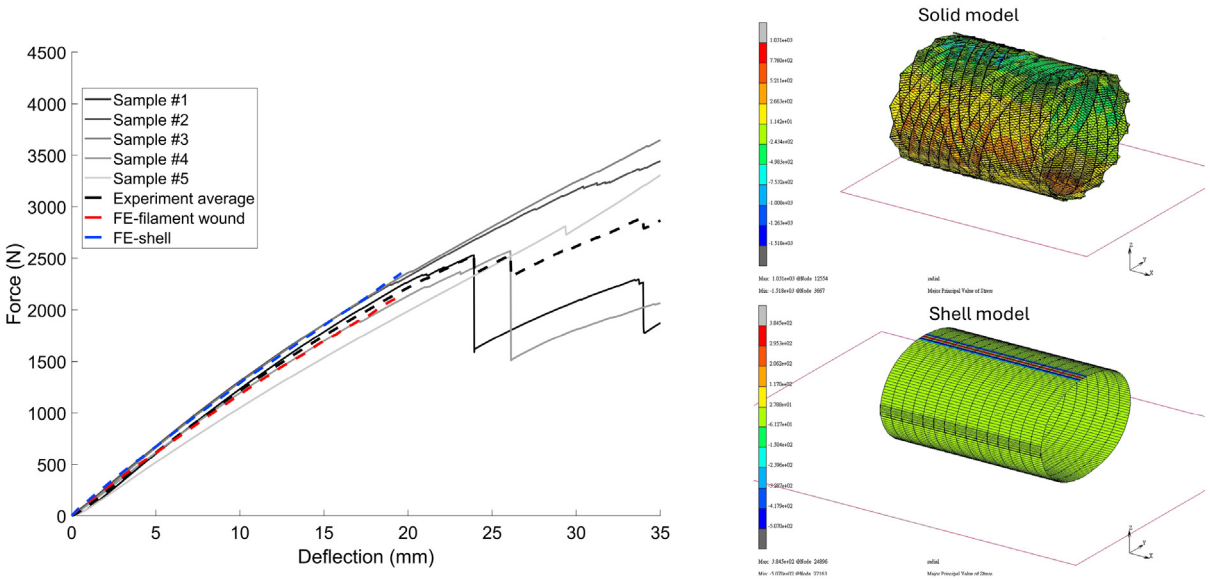

Fig. 3. Left: Force and displacement from experiment vs. FEA (shell & solid models). Right: Stress distribution for shell & solid models.

The resin fills most gaps during curing, allowing resin and fiber to be modeled as composite components with material properties based on fiber volume fraction. The unfilled gaps in the solid model led to conservative results, while the shell model overestimated the stiffness.

During the experiment, two specimens showed a force drop at approximately 24 mm and 26 mm possibly caused by inconsistent wall thickness leading to local fiber failure, as cracks were found in both samples. This behavior was not observed in the other three specimens potentially due to a higher thickness. The solid model did not capture the failure behavior.

Comparing the two models, the solid model is considered better for capturing the behavior of the filament-wound tube average stiffness in the linear region. Even though both models' results were still in the range of scatter, the solid model has a higher potential for predicting failure and damage propagation and capturing all the physical behavior when developed further. For example using Virtual Crack-Closure Technique (VCCT) as the crack initiation, which can be captured by using Digital Image Correlation (DIC) or high-speed camera.

5. Conclusion

This study focused on modeling fiber undulation in filament-wound composite tubes, which were absent in shell elements. The solid model with fiber undulation provided a more conservative stiffness prediction than the shell model. As the undulations are expected to lead to stress concentrations, the solid model is expected to predict the failure behavior and location when improved with failure criteria and damage propagation. Furthermore, it can also be enhanced with the winding at the dome part to create a composite pressure vessel, where the fiber undulation is more frequent and the effects could be more significant.

Declaration of Competing Interest

The authors declare that they have no known competing financial interests or personal relationships that could have appeared to influence the work reported in this paper.

Acknowledgement

The authors would like to acknowledge the funding by the Deutsche Forschungsgemeinschaft (DFG, German Research Foundation) under Germanýs Excellence Strategy – EXC 2163/1 - Sustainable and Energy Efficient Aviation – Project-ID 390881007. Special thanks to Advanced Material Systems Inc., and Dr. Tsai Chia Liang who provided the sample and assisted the experiment.

References

[1] Alam S, Yandek GR, Lee RC, Mabry JM. Design and development of a filament wound composite overwrapped pressure vessel. Compos Part C: Open Access 2020;2:100045. 10.
[2] Nebe M, Asijee TJ, Braun C, van Campen JM, Walther F. Experimental and analytical analysis on the stacking sequence of composite pressure vessels. Compos Struct 2020;247:112429. 9.
[3] Nebe M, Johman A, Braun C, van Campen JM. The effect of stacking sequence and circumferential ply drop locations on the mechanical response of type IV composite pressure vessels subjected to internal pressure: A numerical and experimental study. Compos Struct 2022;294:115585. 8.
[4] Ueda M, Hidaka T, Ichihara N, Yang H, Iwase W, Matsuda T, Morita N, Aoki R, Yokozeki T. Voids in type-IV composite pressure vessels manufactured by a dry filament-winding process. Int J Press Vessels Pip 2024;208:105154. 4.
[5] Almeida JHS, St-Pierre L, Wang Z, Ribeiro ML, Tita V, Amico SC, Castro SG. Design, modeling, optimization, manufacturing and testing of variable-angle filament-wound cylinders. Compos Part B: Eng 2021;225:109224. 11.
[6] Watkins RK, Anderson LR. Structural mechanics of buried pipes. CRC Press; 1999.
[7] Tonatto ML, Forte MM, Tita V, Amico SC. Progressive damage modeling of spiral and ring composite structures for offloading hoses. Mater Des 2016;108:374–82. 10.
[8] Stabla P, Lubecki M, Smolnicki M. The effect of mosaic pattern and winding angle on radially compressed filament-wound CFRP composite tubes. Compos Struct 2022;292:115644. 7.
[9] Lisbôa TV, Almeida JHS, Spickenheuer A, Stommel M, Amico SC, Marczak RJ. FEM updating for damage modeling of composite cylinders under radial compression considering the winding pattern. Thin-Wall Struct 2022;173:108954. 4.
[10] Almeida JHS, Ribeiro ML, Tita V, Amico SC. Damage modeling for carbon fiber/epoxy filament wound composite tubes under radial compression. Compos Struct 2017;160:204–10. 1.
[11] Koussios S. Filament winding: A unified approach. PhD thesis, TU Delft; 2004.
[12] Koussios S, Bergsma OK, Beukers A. Filament winding. Part 1: determination of the wound body related parameters. Compos Part A: Appl Sci Manuf 2004;35:181–95. 2.
[13] Vasiliev VV, Krikanov AA, Razin AF. New generation of filament-wound composite pressure vessels for commercial applications. Compos Struct 2003;62:449–59. 1.
[14] Guo K, Wen L, Xiao J, Lei M, Wang S, Zhang C, Hou X. Design of winding pattern of filament-wound composite pressure vessel with unequal openings based on non-geodesics. J Eng Fibers Fabr 2020;15. p. 1558925020933976, 1.
[15] Wang EL, Gutowski TG. Laps and gaps in thermoplastic composites processing. Compos Manuf 1991;2:69–78. 1.
[16] ASTM International, "ASTM D2412–21. Standard Test Method for Determination of External Loading Characteristics of Plastic Pipe by Parallel-Plate Loading," in ASTM Standards, vol. 08.04.
[17] ASTM International, "ASTM D2122–22: Standard Test Method for Determining Dimensions of Thermoplastic Pipe and Fittings," in ASTM Standards, vol. 08.04.
[18] Toray Composite Materials America, "T700S Datasheet," in Torayca Technical Manual, pp. 18–19; 2020.